

Quantum measurements of coupled systems

L. Fedichkin,¹ M. Shapiro,² and M. I. Dykman^{1,*}¹*Department of Physics and Astronomy, Michigan State University, East Lansing, Michigan 48824, USA*²*Department of Mathematics, Michigan State University, East Lansing, Michigan 48824, USA*

(Received 4 March 2009; published 27 July 2009)

We propose an approach to measuring coupled systems, which gives a parametrically smaller error than the conventional fast projective measurements. The measurement error is due to the excitations being not entirely localized on individual systems even where the excitation energies are different. Our approach combines spectral selectivity of the detector with temporal resolution and uses the ideas of the quantum diffusion theory. The results bear on quantum computing with perpetually coupled qubits.

DOI: [10.1103/PhysRevA.80.012114](https://doi.org/10.1103/PhysRevA.80.012114)

PACS number(s): 03.65.Ta, 03.67.Lx, 03.65.Yz, 85.25.Cp

I. INTRODUCTION

The understanding of quantum measurements has significantly advanced in recent years, in part due to the fast development of quantum information theory [1,2]. Measurements constitute a necessary part of the operation of a quantum computer. In the context of quantum computing, it is often implied that measurements are performed on individual two-state systems, qubits, and that during measurements qubits are isolated from each other. However, in many proposed implementations of quantum computers the qubit-qubit coupling may not be completely turned off. The interest in measuring coupled systems is by no means limited to quantum computing; however, qubits provide a convenient language for formulating the problem.

In a system of coupled qubits (coupled quantum systems) excitations are not entirely localized on individual qubits even where the qubits have different energies. Therefore, if a qubit is excited, a projective measurement on this qubit [3] can miss the excitation. A measurement can also give a false-positive result: the detected excitation may be mostly localized on another qubit but have a tail on the measured qubit. In the context of quantum computing, this is a significant complication since the overall error accumulates with the number of qubits.

A familiar alternative to fast projective measurements is provided by continuous measurements, in which the signal from a qubit is accumulated over time [2]. Continuous measurements are often implemented as quantum nondemolition measurements (QNDMs) in which the quantity to be measured (such as population of the excited state) is preserved while a conjugate quantity (such as phase) is made uncertain. As we will see, the standard QNDMs do not solve the precision problem for interacting qubits.

The goal of the present paper is to find a way of measuring nonresonantly coupled qubits that gives a parametrically smaller error than standard fast or continuous one-qubit measurements. The idea is to combine temporal and spectral selectivities so as to take advantage of different time and energy scales in the system. The proposed measurement is designed for measuring excited states and is continuous.

However, it is not of a QNDM type, both the amplitude and the phase of the excitation wave function are changed.

The problem of measuring coupled qubits is related to the problem of localization. Localization of single-excitation stationary states is well understood since Anderson's work [4] on disordered systems where qubit excitation energies (site energies) ε_n are random. Anderson localization requires that the bandwidth h of the energies ε_n be much larger than the typical nearest-neighbor hopping integral J . One-excitation localization becomes stronger for the same h/J , i.e., the localization length becomes smaller if ε_n are tuned in a regular way so as to suppress resonant excitation transitions. Localizing multiple excitations is far more complicated, because the number of states exponentially increases with the number of excitations. However, at least for a one-dimensional qubit system, by tuning ε_n one can obtain a long "localization lifetime" within which all excitations remain strongly localized on individual qubits, with small wave-function tails on neighboring qubits. The localization lifetime can be as long as $\sim J^{-1}(h/J)^5$ [5,6]; here and below, we set $\hbar=1$.

We propose to detect an excitation by resonantly coupling the measured qubit to a two-level detecting system (DS). If the qubit was initially excited and the DS was in the ground state, the excitation can move to the DS. There, its energy will be transferred to the reservoir and the change in the state of the reservoir will be directly detected. For example, the DS can emit a photon that will be registered by a photodetector. The typical rate of photon emission Γ should largely exceed the rate of resonant (but incoherent) excitation hopping between the qubit and the DS, so that the probability for the excitation to go back to the qubit is small. The rate Γ should also largely exceed the interaction-induced shift of the qubit energy levels. At the same time, Γ should be small compared to the bandwidth of site energies h . Then the qubits adjacent to the measured qubit are not in resonance with the DS, and the rate of excitation transfer from these qubits to the DS is small.

If the above conditions are met, there should be a time interval within which an excitation localized mostly on the measured qubit will be detected with a large probability, whereas excitations localized mostly on neighboring qubits will have a very small probability to trigger a detection signal. As we show, the associated errors are much smaller than in a projective measurement.

State measurements for coupled qubits have been performed with Josephson-junction-based systems, where there

*dykman@pa.msu.edu

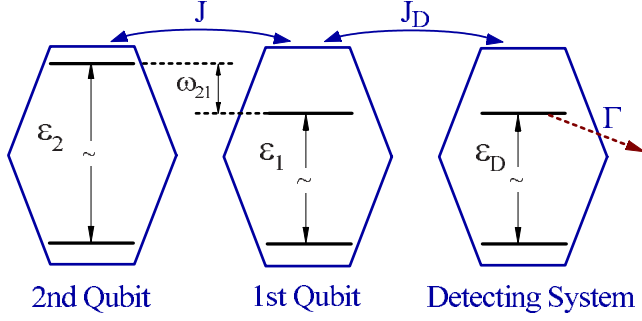


FIG. 1. (Color online) The measurement scheme. Qubits 1 and 2 are not in resonance, but are perpetually coupled, with the coupling constant $J \ll \omega_{21}$, where $\omega_{21} = \varepsilon_2 - \varepsilon_1$ is the level detuning, $\omega_{21} \ll \varepsilon_{1,2}$. The detecting system is resonantly coupled to qubit 1. When an excitation is transferred to the DS, the DS makes a transition to the ground state (for example, with photon emission), which is directly registered. The transition rate Γ exceeds J, J_D , but is small compared to ω_{21} to provide spectral selectivity.

were studied oscillations of excitations between the qubits [7,8]. The oscillations occurred where the qubits were tuned in resonance with each other. The effect of the interaction on measurements in the case of detuned qubits, which is of interest for the present work, was not analyzed. The approach proposed here, which combines spectral and temporal selectivities to achieve high resolution, as well as the goal and the results, are different not only from the standard continuous quantum measurements [2] but also from other types of time-dependent quantum measurements (cf. Refs. [9–12]).

In Sec. II we describe the system of two qubits and a resonant inelastic-scattering-based DS. We identify the range of the relaxation rate of the DS and the qubit parameters where the measurement is most efficient. In Sec. III we study time evolution of the system. We find that the decay rates of stationary states centered at different qubits are strongly different. The detailed theory for one- and two-qubit excitations is given in Appendixes A and B, respectively. Section IV describes how initial states of the system can be efficiently discriminated, and the analytical results are compared with a numerical solution. Section V contains concluding remarks, including an extension of the results to a multiqubit system.

II. MODEL

A. Two-qubit system

We will concentrate on a quantum measurement of two coupled two-level systems (two spin-1/2 particles or two qubits) and then extend the results to a multiqubit system. The system is sketched in Fig. 1. We will assume that the qubit excitation energies (the spin Zeeman energies) $\varepsilon_{1,2}$ largely exceed both the interaction energy J and the energy difference $|\omega_{21}|$, where $\omega_{21} = \varepsilon_2 - \varepsilon_1$; for concreteness, we assume that $\omega_{21} > 0$.

Via the Jordan-Wigner transformation the system can be mapped onto two spinless fermions with Hamiltonian

$$H_S = \sum_{n=1,2} \varepsilon_n a_n^\dagger a_n + \frac{1}{2} J (a_1^\dagger a_2 + a_2^\dagger a_1) + J \Delta a_1^\dagger a_2^\dagger a_2 a_1. \quad (1)$$

Here, the subscript $n=1,2$ enumerates the coupled qubits and a_n, a_n^\dagger are the fermion annihilation and creation opera-

tors. The ground state corresponds to no fermions present. A fermion on site n corresponds to the n th qubit being excited. The parameter J in this language is the hopping integral, whereas $J\Delta$ describes the interaction energy of the excitations.

We will assume that $J \ll \omega_{21}$. In this case the stationary single-particle states of the system $|\psi_{1,2}^{(st)}\rangle$ are strongly localized on site 1 or 2,

$$|\psi_n^{(st)}\rangle = C [|n\rangle - \mu (-1)^n |3-n\rangle] \quad (n=1,2), \quad (2)$$

where $\mu = 2\delta\varepsilon_1/J \approx -J/2\omega_{21}$ and $C = (1 + \mu^2)^{-1/2}$ [$\delta\varepsilon_1 = (\omega_{21} - \sqrt{\omega_{21}^2 + J^2})/2$ is the shift of the energy level ε_1 due to excitation hopping].

Measurements are done by attaching a detector to a qubit, i.e., to the physical system represented by the qubit. For concreteness, we assume that the measured qubit is qubit 1. It is seen from Eq. (2) that, if the measurement is fast projective and the system is in state $|\psi_1^{(st)}\rangle$, the occupation of this state will be detected with an error μ^2 . With probability μ^2 the detector will “click” also if the system is in state $|\psi_2^{(st)}\rangle$. The same error occurs in quasielastic continuous measurements, like measurements with quantum point contacts or tunnel junctions [11,13]. Moreover, the decoherence of the qubit brought about by such measurements, even where its rate is small compared to ω_{21} will lead, for coupled qubits, to excitation spreading over both states $|\psi_{1,2}^{(st)}\rangle$, which will limit the measurement precision.

B. Resonant inelastic-scattering detector

The state of the system can be determined with a higher precision using a detector that involves inelastic transitions. A simple model is provided by a two-level DS which is resonant with qubit 1 (see Fig. 1). The measurement is the registration of a transition of this system from its excited to the ground state; for example, it can be detection of a photon emitted in the transition. The Hamiltonian of the qubit-DS system is

$$H = H_S + \varepsilon_D a_D^\dagger a_D + \frac{1}{2} J_D (a_1^\dagger a_D + a_D^\dagger a_1), \quad (3)$$

where ε_D is the energy of the excited state of the DS and J_D characterizes the coupling of the DS to qubit 1, $J_D \ll \omega_{21}$.

The qubit-DS dynamics can be conveniently analyzed by changing to the rotating frame with a unitary transformation $U(t) = \exp[-i\varepsilon_1 t \sum_{\alpha=1,2,D} a_\alpha^\dagger a_\alpha]$. We assume that relaxation of the DS is due to coupling to a bosonic bath (photons). If this coupling is weak and other standard conditions are met [14], the qubit-DS dynamics in slow time (compared to ε_1^{-1}) is described by the Markovian quantum kinetic equation for the density matrix ρ ,

$$\dot{\rho} = i[\rho, \tilde{H}] - \Gamma (a_D^\dagger a_D \rho - 2a_D \rho a_D^\dagger + \rho a_D^\dagger a_D). \quad (4)$$

Here, $\tilde{H} = H - \varepsilon_1 \sum_{\alpha=1,2,D} a_\alpha^\dagger a_\alpha$ and Γ is the DS decay rate. It is assumed that the bath temperature is $T \ll \varepsilon_D/k_B$, so that there are no thermal transitions of the DS from the ground to the excited state.

Equation (4) should be solved with the initial condition that for $t=0$ the DS is in the ground state whereas the qubits

are in a state to be measured. As a result of the excitation transfer from the qubits, the DS can be excited and then it will make a transition to the ground state. The directly measured quantity is the probability $R(t)$ that such a transition has occurred by time t ,

$$R(t) = 2\Gamma \int_0^t dt \text{Tr}[\rho(t)a_D^\dagger a_D]. \quad (5)$$

It is clear, in particular, that if one of the qubits is excited the excitation will be ultimately fully transferred to the DS and then further transferred to the photon bath, so that $R(t) \rightarrow 1$ for $t \rightarrow \infty$. If on the other hand both qubits are in the ground state, then $R(t)=0$.

As we show, qubit measurements can be efficiently done for

$$\omega_{21} \gg \Gamma \gg J, J_D, |\varepsilon_D - \varepsilon_1|. \quad (6)$$

In this case, there are no oscillations of excitations between the qubits and the DS and time evolution of $R(t)$ is characterized by two strongly different time scales, which makes it possible to determine which of the qubits is excited. The energy detuning $\varepsilon_D - \varepsilon_1$ plays no role, and without loss of generality we can set $\varepsilon_D = \varepsilon_1$. We will start the analysis with the case where there is no more than one excitation on the qubits for $t=0$. Then one can replace \tilde{H} in Eq. (4) with a single-excitation Hamiltonian,

$$\tilde{H} \Rightarrow \omega_{21} a_2^\dagger a_2 + \frac{1}{2}(J a_1^\dagger a_2 + J_D a_1^\dagger a_D + \text{H.c.}). \quad (7)$$

III. TIME EVOLUTION OF THE DENSITY MATRIX

A. One excitation

Evaluating expression (5) requires finding expectation values $\langle a_\beta^\dagger(t) a_\alpha(t) \rangle \equiv \text{Tr} a_\beta^\dagger a_\alpha \rho(t) \equiv \rho_{\alpha\beta}(t)$, where α, β run through the subscripts 1, 2, D . The matrix elements $\rho_{\alpha\beta} = \rho_{\beta\alpha}^*$ satisfy a system of nine linear equations that follow from the operator equations (4) and (7). This system of equations is closed; the matrix elements $\rho_{\alpha\beta}$ do not mix with the expectation values $\langle a_\alpha(t) \rangle, \langle a_\alpha^\dagger(t) \rangle$.

The solution of the equations for $\rho_{\alpha\beta}(t)$ and the analysis of the signal $R(t)$ are simplified in range (6). The relaxation rate of the matrix elements $\rho_{D\alpha}$ that involve the DS is $\sim \Gamma$. For $\Gamma \gg J_D, J$ this rate is faster than other relaxation rates, as explained below (see Appendix A for details), and therefore over time Γ^{-1} the matrix elements $\rho_{D\alpha}$ reach their quasistationary values.

Relaxation of the population ρ_{11} of qubit 1, on the other hand, is determined by the excitation transfer from site 1 to the DS. This transfer is similar to quantum diffusion of weakly coupled defects in solids within narrow bands of translational motion [15] or defect reorientation between equivalent positions in an elementary cell [16]. It is characterized by the rate

$$W_1 = J_D^2/2\Gamma, \quad W_1 \ll \Gamma. \quad (8)$$

Equation (8) can be readily understood in terms of the Fermi golden rule: this is a transition rate from qubit 1 to the DS

induced by the interaction $\propto J_D$, with Γ being the characteristic bandwidth of final states and Γ^{-1} being the density of states at the band center, respectively. The rate W_1 describes the relaxation of an excitation localized initially in state $|\psi_1^{(st)}\rangle$.

If the excitation is localized mostly on qubit 2 and has energy $\approx \omega_{21}$, its decay rate is much smaller. The decay can be thought of as due to the interaction of qubit 2 with the DS, which is mediated (nonresonantly) by qubit 1. Therefore the effective interaction energy is $\approx J J_D / 2\omega_{21}$. The effective density of final states is determined by the tail of the density of states of the DS at frequency $\omega_{21} \gg \Gamma$. For the exponential in time relaxation described by Eq. (4) the density of states is Lorentzian, and on the tail at frequency ω_{21} it is $\sim \Gamma / \omega_{21}^2$. Therefore the expected decay rate W_2 is

$$W_2 = J^2 J_D^2 \Gamma / 8\omega_{21}^4, \quad W_2 \ll W_1. \quad (9)$$

It follows from the result of Appendix A that, if for $t=0$ the two-qubit system is in stationary state $|\psi_n^{(st)}\rangle$ ($n=1, 2$), the probability $R_n(t)$ to receive a signal by time t is

$$R_n(t) = 1 - \exp(-W_n t) \quad (n=1, 2). \quad (10)$$

The strong difference between $W_{1,2}$ and Γ justifies the assumption that $\rho_{D\alpha}$ reaches a quasistationary value before the populations ρ_{11}, ρ_{22} change. The full theory of qubit relaxation is described in Appendix A.

B. Two excitations

The above analysis can be readily extended to the case where both qubits 1 and 2 are initially in the excited state, i.e., initially there are two spinless fermions on sites 1 and 2. We will assume that the interaction between the excitations (fermions) $J\Delta$ is not strong, so that $|J\Delta| \ll \Gamma$. The qualitative picture of the dynamics of the system then is simple. First, over time $\sim \Gamma^{-1}$ there is established a quasistationary ‘‘quantum diffusion current’’ from qubit 1 to the DS, which is determined by the transition rate W_1 and is equal to $W_1 \rho_{11}(t)$. It drains stationary state $|\psi_1^{(st)}\rangle$ over time $\sim W_1^{-1}$. The presence of an excitation (fermion) in state $|\psi_2^{(st)}\rangle$ only weakly affects this current because of the large energy difference of the states ω_{21} . After state $|\psi_1^{(st)}\rangle$ is emptied, further evolution corresponds to the single-excitation decay of state $|\psi_2^{(st)}\rangle$. Therefore the overall signal should be

$$R^{(2e)}(t) = R_1(t) + R_2(t) = 2 - e^{-W_1 t} - e^{-W_2 t}. \quad (11)$$

A detailed derivation of this expression is given in Appendix B. It is clear from the above analysis that the most interesting problem is to distinguish which of the stationary states $|\psi_{1,2}^{(st)}\rangle$ is initially occupied; the situation where both of them are occupied is simpler.

IV. RESOLVING ONE-EXCITATION STATES FROM TIME-DEPENDENT MEASUREMENTS

The rates W_1 and W_2 of signal accumulation for different initially occupied one-excitation states are parametrically different. This enables a high-accuracy discrimination between the states using a resonant DS. The results for time

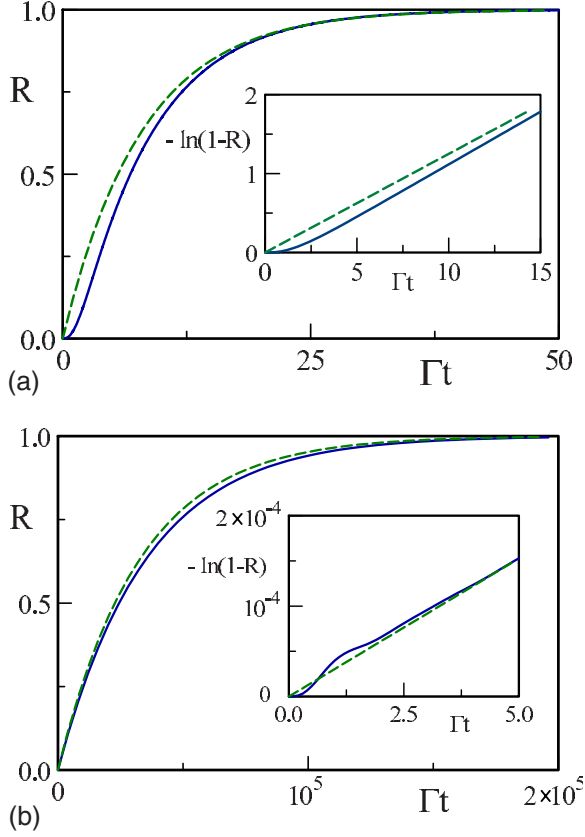


FIG. 2. (Color online) Time dependence of the probability to detect a signal for the two-qubit system being initially in the stationary states (a) $|\psi_1^{(st)}\rangle$ and (b) $|\psi_2^{(st)}\rangle$. Note the difference of the time scales. The parameters are $\omega_{21}/\Gamma=4, J/\Gamma=J_D/\Gamma=1/2$. The solid and the dashed lines show, respectively, the numerical solution of the master equation and the asymptotic expressions (10) for the limiting case $\omega_{21} \gg \Gamma \gg J, J_D$. The insets show $|\ln[1-R_1(t)]|$ for small time, where the difference between the numerical and the asymptotic expressions is most pronounced.

evolution of the signals $R(t)$ obtained by a numerical solution of the system of equations for the matrix elements $\rho_{\alpha\beta}$ are shown in Figs. 2 and 3. The figures refer, respectively, to the cases where the system of qubits is initially in one of the eigenstates $|\psi_{1,2}^{(st)}\rangle$ and in a mixed state. It is seen from the figures that, even where the parameter ratios Γ/ω_{21} and $J/\Gamma, J_D/\Gamma$ are not particularly small, the results are well described by the asymptotic expressions (10).

The adiabatic expressions (10) do not describe how the matrix elements $\rho_{\alpha\beta}$ approach their adiabatic values, and thus they do not describe the evolution of R for $t \lesssim \Gamma^{-1}$. Since the DS is initially in the ground state, it follows from Eqs. (4) and (5) that $R(t) \propto t^2$ for $t \rightarrow 0$ in contrast to $R \propto t$ as predicted by Eq. (10).

Breaking of the adiabaticity for short times explains the shifts of the asymptotic curves (10) with respect to the numerically calculated curves in Fig. 2. For the initially occupied state $|\psi_1^{(st)}\rangle$, adiabaticity is established over time $t \sim \Gamma^{-1}$; this is the relaxation time of the matrix elements $\rho_{\alpha D}, \rho_{D\alpha}$. Then from Eq. (10) the shift should be $\sim W_1/\Gamma$, which agrees with Fig. 2(a). For state $|\psi_2^{(st)}\rangle$ the exponential decay of R_2 [Eq. (10)] is obtained in the double-adiabatic

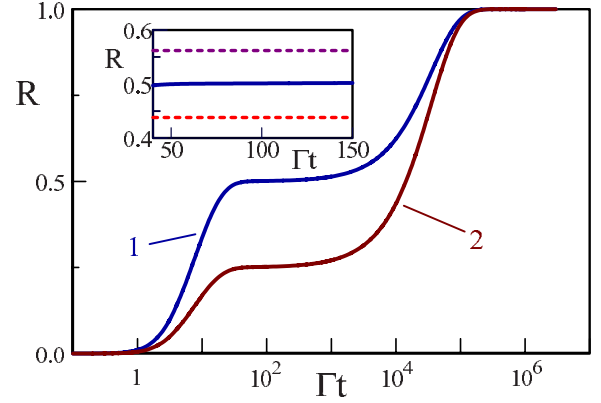


FIG. 3. (Color online) Time dependence of the probability to detect a signal for the two-qubit system being initially in a superposition of stationary states $|\psi(0)\rangle = \cos \theta |\psi_1^{(st)}\rangle + \sin \theta |\psi_2^{(st)}\rangle$. Curves 1 and 2 present the numerical solution of the master equation and refer to $\theta = \pi/4$ and $\pi/3$, respectively. The parameters of the qubits and the DS are the same as in Fig. 2. Inset: the solid line shows $R(t)$ for $\theta = \pm \pi/4$ (state population $P_1 = 1/2$) in the optimal time range (14), the dashed lines show the results of fast projective measurements on qubit 1, $|\langle 1 | \psi(0) \rangle|^2$, for $\theta = \pm \pi/4$, which significantly differ from P_1 .

approximation, which exploits the interrelation between the relaxation rates $\Gamma \gg W_1 \gg W_2$. The adiabatic regime is formed over time $\sim W_1^{-1}$, and the shift of the numerical curve with respect to the asymptotic one is $\sim W_2/W_1$, which agrees with Fig. 2(b).

If the initial state of the system $|\psi(0)\rangle$ is a superposition of stationary states $|\psi_1^{(st)}\rangle$ and $|\psi_2^{(st)}\rangle$, for $\Gamma t \gg 1$ the signal $R(t)$ is the appropriately weighted superposition of the signals $R_1(t)$ and $R_2(t)$ (see Appendix A),

$$R(t) \approx P_1[1 - \exp(-W_1 t)] + P_2[1 - \exp(-W_2 t)],$$

$$P_n = |\langle \psi(0) | \psi_n^{(st)} \rangle|^2. \quad (12)$$

Here, $P_{1,2}$ are the initial populations of the stationary states. We note that $P_1 + P_2 \neq 1$ in the general case where the initial state is a superposition of the ground and one- or two-excitation states.

Over time $\sim W_1^{-1}$ the function $R(t)$ approaches the population P_1 of state $|\psi_1^{(st)}\rangle$. Further change in $R(t)$ occurs over a much longer time $\sim W_2^{-1}$. This is seen in Fig. 3. As explained in Appendix A, a contribution to $R(t)$ from fast-oscillating terms $\propto \exp(\pm i\omega_{21}t)$ in the density matrix is small compared to $(J/\omega_{21})^2$: for $\Gamma t \gg 1$ the corresponding correction to Eq. (12) is $\lesssim JJ_D^2/4\omega_{21}^3 \text{Re} \rho_{12}(0) \ll J^2/4\omega_{21}^2$ (we assume $J_D \sim J$).

From Eq. (12), in a broad time interval an error in the measured population of state $|\psi_1^{(st)}\rangle$ is smaller than in a fast projective measurement. If the initial state is $|\psi(0)\rangle = P_1^{1/2} |\psi_1^{(st)}\rangle + P_2^{1/2} \exp(i\phi) |\psi_2^{(st)}\rangle$ (plus a possible contribution from the ground state of the qubits), a fast projective measurement on qubit 1 gives

$$|\langle 1|\psi(0)\rangle|^2 \approx \left(1 - \frac{J^2}{4\omega_{21}^2}\right) \left|P_1^{1/2} + P_2^{1/2} e^{i\phi} \frac{J}{2\omega_{21}}\right|^2. \quad (13)$$

This differs from P_1 by $\sim J/\omega_{21}$ for $P_1 \sim P_2$; in the case of strongly different populations where P_1/P_2 or P_2/P_1 is $\lesssim J^2/\omega_{21}^2$ the difference becomes $\sim J^2/\omega_{21}^2$. The proposed measurement gives a parametrically smaller error. We have

$$|R(t) - P_1| \ll \frac{J^2}{4\omega_{21}^2} \quad \text{for } e^{-W_1 t}, W_2 t \ll \frac{J^2}{4\omega_{21}^2}. \quad (14)$$

In the explicit form, the time interval for a high-accuracy measurement of state $|\psi_1^{(st)}\rangle$ is determined by the condition $2 \ln(2\omega_{21}/J) \ll W_1 t \ll (\omega_{21}/\Gamma)^2$. This condition is easy to satisfy in the parameter range (6). The difference between the proposed approach and a fast projective measurement is illustrated in the inset in Fig. 3.

The proposed approach can be compared with a seemingly simpler scheme in which one directly turns on the coupling of qubit 1 to a thermal reservoir and detects the emitted excitation. The scheme is similar to the one implemented in Josephson phase qubits [7,8] where qubit decay was effectively turned on by reducing the appropriate tunnel barrier. This is essentially a “fast” projective measurement of qubit 1 with duration equal to qubit lifetime Γ^{-1} . For large detuning, $\omega_{21} \gg \Gamma, J$, the decay rate of the stationary state localized mostly on qubit 2 can be estimated, following the arguments of Sec. III, as $\sim J^2\Gamma/\omega_{21}^2$. Therefore, if the system is initially in state $|\psi_2^{(st)}\rangle$, over time Γ^{-1} the detector will click with probability $\sim (J/\omega_{21})^2\Gamma \sim (J/\omega_{21})^2$. This is an expected error of a projective measurement of coupled qubits; in our approach the error is much smaller. We note that in the Josephson phase qubits system [7,8] two-qubit measurements are additionally complicated by cross talk [17].

V. CONCLUSIONS

We have demonstrated that a state of two coupled two-level systems (qubits), which are detuned from each other, can be determined with an accuracy much higher than that of a fast projective measurement. This is accomplished by combining frequency and temporal selectivities. The detector is tuned in resonance with the qubit to which it is directly coupled. When the detector relaxation rate Γ is larger than the coupling J, J_D , but smaller than the energy difference between the qubits ω_{21} , the overall relaxation of the system is characterized by two strongly different time scales. One is the reciprocal decay rate of the excited stationary state localized mostly on the resonant qubit $W_1^{-1} = 2\Gamma/J_D^2$. The other is the parametrically larger reciprocal decay rate of the excited stationary state localized mostly on the nonresonant qubit $W_2^{-1} = 8\omega_{21}^4/(JJ_D)^2\Gamma$. This makes it possible to discriminate between the states using time-dependent measurements.

The measurement requires turning on the interaction between the measured qubit and the DS. This can be done either directly or, often more conveniently, by tuning the DS in resonance with the qubit. The required precision is determined by the decay rate of the DS Γ . Moreover, one can slowly sweep the DS energy level through the qubit energy,

so that the energies stay in resonance (to the accuracy of $\sim \Gamma$) for a time $\geq W_1^{-1}$.

The results can be generalized to the case of a many-qubit system. Of particular interest is a qubit chain with Hamiltonian

$$H = \sum_n \varepsilon_n a_n^\dagger a_n + \frac{1}{2} J \sum_n (a_n^\dagger a_{n+1} + a_{n+1}^\dagger a_n) + J\Delta \sum_n a_n^\dagger a_{n+1}^\dagger a_{n+1} a_n, \quad (15)$$

which is an immediate extension of the two-qubit Hamiltonian (1). As mentioned in Sec. I, for appropriately tuned site energies ε_n all many-particle excitations in such a chain remain localized for a long time, which scales as a high power of h/J (h is the typical bandwidth of energies ε_n) [5,6]. However, excitations are not fully localized on individual sites; in (quasi)stationary states the tails of their wave functions on neighboring sites are $\sim J/h$.

Following the proposed method, to determine whether there is an excitation localized in a quasistationary state centered at a given qubit, one should couple this qubit resonantly to a DS. The excitation will be detected over time $\sim W_1^{-1}$. Excitations localized mostly on neighboring qubits will not affect the measurement as long as the duration of the measurement is small compared to W_2^{-1} . The reduction in the measurement error compared to a fast projective measurement facilitates scalable quantum computing with perpetually coupled qubits.

We are grateful to A. Korotkov and F. Wilhelm for helpful discussions. This work was supported in part by the National Science Foundation through Grants No. PHY-0555346 and No. EMT/QIS-0829854.

APPENDIX A: ADIABATIC APPROXIMATION

Here we consider the dynamics of a two-qubit system coupled to the DS where there is initially one excitation on the qubits. The dynamics is described by Eqs. (4) and (7), which can be written as nine linear first-order equations for the matrix elements $\rho_{\alpha\beta}(t) = \langle a_\beta^\dagger(t) a_\alpha(t) \rangle$. Formally one can solve these equations by finding the corresponding eigenvalues and eigenfunctions. For a strong inequality between the transition frequency ω_{21} , on one hand, and the decay rate Γ and the hopping integrals J, J_D , on the other hand, the eigenvalues can be separated into those corresponding to fast weakly damped oscillations and to slow evolution. There are four “fast” eigenvalues with imaginary part close to $\pm\omega_{21}$. In particular, as seen from Eq. (4), to zeroth order in J, J_D we have $\rho_{12}, \rho_{D2} \propto \exp(i\omega_{21}t)$. In turn, where $\Gamma \gg J, J_D$, among the remaining “slow” eigenvalues there are three with real parts $\propto -\Gamma$; indeed, $\rho_{DD} \propto \exp(-2\Gamma t)$ and $\rho_{D1} = \rho_{1D}^* \propto \exp(-\Gamma t)$, to zeroth order in J, J_D . The remaining two “slow” eigenvalues, as we will show, are given by Eqs. (8) and (9).

The analysis of slow dynamics can be done in the adiabatic approximation. Since the relaxation rate of $\rho_{D\alpha}$ ($\alpha=1, 2, D$) is $\propto \Gamma$, over time $t \gg \Gamma^{-1}$ these matrix elements reach quasistationary values. These values adiabatically fol-

low the slowly evolving matrix elements ρ_{nm} , where roman subscripts $n, m=1, 2$. In particular, by noting that $(\partial/\partial t)\sum_{\alpha}\rho_{\alpha\alpha}=-2\Gamma\rho_{DD}$ we obtain

$$\rho_{DD} \approx -(\dot{\rho}_{11} + \dot{\rho}_{22})/2\Gamma. \quad (\text{A1})$$

1. Evolution of the one-excitation stationary state resonant with the DS

We assume first that the system is in the stationary state $|\psi_1^{(st)}\rangle$, which has energy close to the DS energy. In this case, for $t=0$ we have $\rho_{11} \gg \rho_{22} \approx (J/\omega_{21})^2\rho_{11}$ and all off-diagonal matrix elements $\rho_{\alpha\beta}$ with $\alpha \neq \beta$ are small compared to ρ_{11} . As we will see, this hierarchy persists for $t > 0$ as well. For $t \gg \Gamma^{-1}$, to the leading order in J, J_D , we have $\rho_{D1} \approx i(J_D/2\Gamma)(\rho_{DD} - \rho_{11}) + i(J/2\Gamma)\rho_{D2}$ and $\rho_{DD} \approx -(J_D/2\Gamma)\text{Im}\rho_{D1}$. Substituting ρ_{D1} into the equation for $\dot{\rho}_{11}$ and eliminating ρ_{DD} , we obtain, to the leading order,

$$\begin{aligned} \dot{\rho}_{11} &\approx -W_1\rho_{11} + \Delta_{11}, \\ \Delta_{11} &= \frac{1}{2}iJ(\rho_{12} - \rho_{21}) + \frac{JJ_D}{2\Gamma}\text{Re}\rho_{D2}, \end{aligned} \quad (\text{A2})$$

where W_1 is given by Eq. (8); as seen from Eq. (A2), this is the relaxation rate of ρ_{11} . In agreement with the adiabaticity assumption, we have $W_1 \leq \Gamma$.

To find the time evolution of ρ_{22} , one has to use the equations

$$\begin{aligned} \dot{\rho}_{12} &= i\omega_{21}\rho_{12} + \frac{1}{2}iJ(\rho_{11} - \rho_{22}) - \frac{1}{2}iJ_D\rho_{D2}, \\ \dot{\rho}_{22} &= -\frac{1}{2}iJ(\rho_{12} - \rho_{21}) \end{aligned} \quad (\text{A3})$$

that immediately follow from the operator equation (4). Using the equation for $\dot{\rho}_{D2}$ that also follows from Eq. (4) and the expression for ρ_{D1} given above, one can show that, for $\rho_{11} \gg \rho_{22}$, $\rho_{D2} \approx i(JJ_D/4\omega_{21}\Gamma)\rho_{11}$ [cf. Eq. (A4) below]. This expression should be substituted into Eqs. (A3) for ρ_{12} . One then obtains $\text{Im}\rho_{12} \approx (J/4\omega_{21}^2)\dot{\rho}_{11}$. Then from the second equation in Eqs. (A3), $\dot{\rho}_{22} \approx (J/2\omega_{21})^2\dot{\rho}_{11}$. Therefore, if the system is initially in the stationary state $|\psi_1^{(st)}\rangle$, the relation between $\rho_{22}(t)$ and $\rho_{11}(t)$ remains unchanged, to the leading order in J .

From Eqs. (5), (A1), and (A2) we see that, if the two-qubit system is initially in the stationary state $|\psi_1^{(st)}\rangle$, the probability to have detected this state by time t is $R_1(t) = 1 - \exp(-W_1 t)$. We use this expression in Eq. (10).

2. Evolution of the nonresonant one-excitation stationary state

If the system is initially in state $|\psi_2^{(st)}\rangle$, we have $\rho_{11} \ll \rho_{22}$. Then it is important to keep track of higher-order corrections in J/ω_{21} in the equations for $\rho_{\alpha\beta}$. In particular, in the adiabatic approximation one has to write $\rho_{D2}(t)$ as

$$\rho_{D2}(t) \approx [2(\omega_{21} + i\Gamma)]^{-1} \left[J_D\rho_{12}(t) + i\frac{JJ_D}{2\Gamma}\rho_{11}(t) \right]. \quad (\text{A4})$$

The decay rate of $\rho_{12}(t)$ can be obtained by substituting Eq. (A4) into Eqs. (A3) for $\dot{\rho}_{12}$, which gives the decay rate as

$(J_D/2\omega_{21})^2\Gamma$. This rate is small compared to the decay rate Γ of ρ_{D2} , justifying the adiabatic approximation used in Eq. (A4). At the same time, as we will see, it is large compared to the decay rate of ρ_{22} .

To describe the decay of ρ_{22} , we substitute the adiabatic solution of Eqs. (A3) for $\text{Im}\rho_{12}$ [with account taken of Eq. (A4)] into Eqs. (A3) for ρ_{22} . This gives

$$\dot{\rho}_{22} \approx -W_2\rho_{22}, \quad (\text{A5})$$

with the decay rate W_2 of the form of Eq. (9).

Noting that $\text{Re}\rho_{12} \approx (J/2\omega_{21})\rho_{22}$, we obtain from Eqs. (A2) and (A4) that, for time $t \gg W_1^{-1}$, we have $\rho_{11}(t) \approx (J/2\omega_{21})^2\rho_{22}(t)$. Then from Eqs. (5), (A1), and (A5), we obtain the explicit expression (10) for the probability to detect state $|\psi_2^{(st)}\rangle$ in time t .

If initially the system is in a superposition of states $|\psi_1^{(st)}\rangle$ and $|\psi_2^{(st)}\rangle$, the density matrix along with slowly varying (on time ω_{21}^{-1}) terms has terms that contain fast oscillating factors $\propto \exp(\pm i\omega_{21}t)$. One can show that, for $t \geq \Gamma^{-1}$, their decay is controlled by the decay of the fast-oscillating component $\rho_{12}^{(f)}(t) = [\rho_{21}^{(f)}(t)]^*$, which is characterized by the factor $\exp(-W_1 t/2)$. The corresponding fast-oscillating term in the population of the excited state of the DS is $\rho_{DD}^{(f)}(t) \sim i(JJ_D^2/8\Gamma\omega_{21}^2)\rho_{12}^{(f)}(t) + \text{c.c.}$ Therefore the contribution of the fast-oscillating terms to the observed probability $R(t)$ is $\lesssim (JJ_D^2/2\omega_{21}^3)\text{Re}\rho_{12}(0)$. It is small compared to the measurement error $\sim J^2/\omega_{21}^2$ that we want to overcome.

APPENDIX B: DYNAMICS OF THE TWO-EXCITATION STATE

In the presence of two excitations, along with two-particle matrix elements $\rho_{\alpha\beta}(t) = \langle a_{\beta}^{\dagger}(t)a_{\alpha}(t) \rangle$, the dynamics of the system is characterized by four-particle matrix elements $\rho_{\alpha\beta\gamma\delta}(t) = \langle a_{\delta}^{\dagger}(t)a_{\gamma}^{\dagger}(t)a_{\beta}(t)a_{\alpha}(t) \rangle$. For a two-qubit system coupled to a DS, each greek subscript runs through three values. The dynamics is described by a set of 18 linear differential equations that follow from the equation of motion for the density matrix in the operator form (4): nine equations for $\dot{\rho}_{\alpha\beta}$ and nine equations for $\dot{\rho}_{\alpha\beta\gamma\delta}$. The number of independent matrix elements follows from the permutation symmetry $\delta \rightleftharpoons \gamma, \beta \rightleftharpoons \alpha$ (a permutation is accompanied by a sign change) and the commutation relations for the fermion operators $a_{\alpha}, a_{\alpha}^{\dagger}$. The system of equations for the four-particle matrix elements is closed: $\rho_{\alpha\beta\gamma\delta}$ are expressed in terms of each other, whereas their evolution affects the two-particle matrix elements $\rho_{\alpha\beta}$.

We will again use the adiabatic approximation to study the dynamics and will start with the matrix elements $\rho_{\alpha\beta\gamma\delta}$. Formally, their time evolution is determined by the eigenvalues of the system of equations for ρ . Four of these eigenvalues have imaginary part $\approx \pm \omega_{21}$ and correspond to fast oscillations. In the limit $J \rightarrow 0$ the corresponding eigenvectors $\rho_{\alpha\beta\gamma\delta}$ have one of the subscripts equal to 2, whereas other three subscripts are two 1 and one D or two D and one 1. Among the eigenvalues that describe slow motion, there are two $\approx -\Gamma$ and two $\approx -2\Gamma$. In the limit $J \rightarrow 0$ the corresponding eigenvectors are ρ_{D212}, ρ_{12D2} , and ρ_{nmDD} ($n=1, 2$). Only one eigenvector controls the evolution of the four-particle

matrix elements on times longer than Γ^{-1} ; the leading-order term in this eigenvector is ρ_{1221} .

Over time $t \geq \Gamma^{-1}$ the matrix elements $\rho_{\alpha\beta\gamma\delta}$ reach their quasistationary values which are determined by $\rho_{1221}(t)$. They can be found by disregarding $\dot{\rho}_{\alpha\beta\gamma\delta}$ in all equations except for the equation for $\dot{\rho}_{1221}$. This gives, in particular,

$$\rho_{D221}(t) \approx -\frac{iJ_D}{2\Gamma}\rho_{1221}(t), \quad \dot{\rho}_{1221} \approx -W_1\rho_{1221}, \quad (\text{B1})$$

whereas $\rho_{1D21} \approx i(JJ_D/4\omega_{21}\Gamma)\rho_{1221}$. It is seen from Eq. (B1) that all slowly varying components of $\rho_{\alpha\beta\gamma\delta}$ decay to zero over time $\sim W_1^{-1}$. This makes sense since this is the time over which the occupation of state $|\psi_1^{(sb)}\rangle$ decays, after which there

remains only one excitation in the system. The fast-oscillating components of $\rho_{\alpha\beta\gamma\delta}$ decay even faster, over time Γ^{-1} .

The signal $R(t)$ [Eq. (5)] is determined by the two-particle matrix element $\rho_{DD}(t)$. One can show that, in the time range $t \geq \Gamma^{-1}$, the major result of the interaction between the excitations on the two-particle matrix elements is that $\rho_{D1}(t)$ is incremented by $\approx (iJ\Delta/\Gamma)\rho_{D221}(t)$ and the slow part of $\rho_{D2}(t)$ is incremented by $\approx -(J\Delta/\omega_{21})\rho_{1D21}(t)$. The first of these corrections drops out from the expression for ρ_{DD} , whereas the contribution from the second is small compared to $(J/\omega_{21})^2$. Therefore, to the accuracy we are interested in, the interaction between excitations does not affect measurements in the proposed approach.

-
- [1] J. Clarke and F. K. Wilhelm, *Nature (London)* **453**, 1031 (2008).
 - [2] A. A. Clerk, M. H. Devoret, S. M. Girvin, F. Marquardt, and R. J. Schoelkopf, e-print arXiv:0810.4729.
 - [3] J. von Neumann, *Mathematical Foundations of Quantum Mechanics* (Princeton University Press, Princeton, NJ, 1983).
 - [4] P. W. Anderson, *Phys. Rev.* **109**, 1492 (1958).
 - [5] L. F. Santos, M. I. Dykman, M. Shapiro, and F. M. Izrailev, *Phys. Rev. A* **71**, 012317 (2005).
 - [6] M. I. Dykman, L. F. Santos, and M. Shapiro, *J. Opt. B: Quantum Semiclassical Opt.* **7**, S363 (2005).
 - [7] R. McDermott, R. W. Simmonds, M. Steffen, K. B. Cooper, K. Cicak, K. D. Osborn, S. Oh, D. P. Pappas, and J. M. Martinis, *Science* **307**, 1299 (2005).
 - [8] N. Katz *et al.*, *Science* **312**, 1498 (2006).
 - [9] M. Heiblum, *Phys. Scr.*, T **68**, 27 (1996).
 - [10] S. Han, Y. Yu, X. Chu, S.-I. Chu, and Z. Wang, *Science* **293**, 1457 (2001).
 - [11] A. N. Korotkov, *Phys. Rev. B* **63**, 115403 (2001).
 - [12] S. Ashhab, J. Q. You, and F. Nori, *Phys. Rev. A* **79**, 032317 (2009).
 - [13] S. A. Gurvitz, *Phys. Rev. B* **56**, 15215 (1997).
 - [14] E. Lifshitz and L. Pitaevskii, *Physical Kinetics* (Butterworth-Heinemann Ltd., Oxford, 1981).
 - [15] Y. Kagan and M. I. Klinger, *J. Phys. C* **7**, 2791 (1974).
 - [16] M. I. Dykman and G. G. Tarasov, *Zh. Eksp. Teor. Fiz.* **74**, 1061 (1978) [*Sov. Phys. JETP* **47**, 557 (1978)].
 - [17] A. G. Kofman, Q. Zhang, J. M. Martinis, and A. N. Korotkov, *Phys. Rev. B* **75**, 014524 (2007).